Sub-10 nm structures on silicon by thermal dewetting of platinum

2010 Nanotechnology 21 505301

(http://iopscience.iop.org/0957-4484/21/50/505301)

Nanotechnology **21** (2010) 505301 (7pp) doi:10.1088/0957-4484/21/50/505301

Sub-10 nm structures on silicon by thermal dewetting of platinum

Sebastian Strobel[1], **Christopher Kirkendall**[1,2], **Jae-Byum Chang**[1] **and Karl K Berggren**[1]

[1] Department of Electrical Engineering and Computer Science, Massachusetts Institute of Technology, Cambridge, MA 02139, USA
[2] College of Engineering, University of Missouri, Columbia, MO 65211, USA

E-mail: berggren@mit.edu

Received 31 August 2010, in final form 21 October 2010
Published 22 November 2010
Online at stacks.iop.org/Nano/21/505301

Abstract
A study of the dewetting behavior of platinum-thin-films on silicon was carried out to determine how variation of dewetting parameters affects the evolution of film morphology and to pinpoint which parameters yielded the smallest, most circular features. Platinum film thickness as well as dewetting time and temperature were varied and the film morphology characterized by means of scanning electron microscopy (SEM) analysis. Two different pathways of dewetting predicted in the literature (Vrij 1966 *Discuss. Faraday Soc.* **42** 23, Becker *et al* 2003 *Nat. Mater.* **2** 59–63) were observed. Depending on the initial criteria, restructuring of the film occurred via hole or droplet formation. With increased annealing time, a transition from an intermediate network structure to separated islands occurred. In addition, the formation of multilayered films, silicide crystals and nanowires occurred for certain parameters. Nevertheless, the dewetting behavior witnessed could be related to physical processes. Droplets with a mean diameter of 9 nm were formed by using a 1.5 nm thick platinum film annealed at 800 °C for 30 s. To demonstrate the suitability of the annealed films for further processing, we then used the dewetted films as masks for reactive ion etching to transfer the pattern into the silicon substrate, forming tapered nanopillars.

1. Introduction

Thermal dewetting of thin platinum (Pt) films offers a simple, low cost method of producing a textured surface topography. Dewetting occurs when thin films on a solid substrate are heated, inducing clustering of the film. Lee and Kim already employed thermal dewetting in the creation of etch masks for fabrication of semiconductor nanostructures on a larger length scale [3]. The same method was also used by Lee *et al* [4] to produce antireflective surfaces. While these works demonstrated the advantages of thermal dewetting as a method for large-scale nanostructuring, the smallest features produced were ∼60 nm in diameter. The current research characterizes the dewetting behavior of platinum-thin-films on a silicon (Si) substrate with the focus on understanding the limit of structure-dimension scaling. We determined process parameters that resulted in structures with sub-10 nm mean diameter. The dewetted pattern was then used as an etch mask to form tapered nanopillars in Si. Moreover, different evolutionary paths of dewetting, i.e. dewetting via droplet or hole formation, were obtained and related to theory. In addition, we observed more unusual phenomena such as nanowire growth. In this study, we relate the theoretical model of dewetting to experiments performed on metal films with different thickness.

2. Theory

To understand the experimental results in more detail, we first briefly introduce the physical processes and the possible evolutionary pathways of dewetting. The structural evolution of a film during dewetting depends critically on the behavior which results in a lower free energy. The free energy of a film, or more exactly the total excess intermolecular interaction free energy per unit area (ΔG), depends on the free energies of cohesion of the substrate, film, and bounding media, as well as on the energies of interaction between them. These energies result from various long- and short-range forces including dispersion, polar, induction, and hydrogen bonding effects [5].

Based on the change of the energy, the film diffusivity is defined as $\partial^2(\Delta G)/\partial h^2$.

The prior literature identifies two central mechanisms underlying dewetting phenomena: nucleation and spinodal dewetting [1, 2, 6–8]. In spinodal dewetting (instability driven), thermally induced surface perturbations experience amplification via dispersion forces, engendering spontaneous rupture of the thin film. Under these conditions, negative diffusion ($\partial^2\Delta G/\partial h^2 < 0$) promotes flow from thinner to thicker regions and a bicontinuous pattern of hills and valleys results [9]. While spinodal dewetting dominates in thinner films and can only take place if $\partial^2\Delta G/\partial h^2 < 0$, nucleation is the main contribution for films whose thickness exceeds a certain threshold value. Above this threshold, dewetting can only occur via nucleation [7]. Nucleation is characterized by chemical/physical heterogeneity which spurs hole formation and growth in the film. If the holes are initiated by defects it is called heterogeneous nucleation.

Sharma and Khanna have performed a series of simulations modeling the nonlinear thin film equation [8–10]. They have found that beyond the earliest phases of growth, the shape of the free energy of interaction (ΔG) and the initial location of the film thickness on this curve largely determine dewetting patterns. In a system where both long- and short-range forces compete, two distinct ΔG behaviors may arise: either a long-range repulsion coupled with a short-range attraction (Sharma and Khanna called it a type IV system) or the opposite scenario of a long-range attraction and short-range repulsion (type II system).

Our investigated apolar system, metal on silicon with a thin oxide coating, is a type IV system. The high-energy Si substrate generates a long-range repulsion (stabilizing), while the low-energy coating produces a shorter-range attraction (destabilizing) [11]. Beyond a critical thickness the film becomes metastable as the long-range repulsion dominates.

Regarding the influence of initial film thickness location along the ΔG profile, Sharma identified two sequences of evolution in the analysis of type IV systems [8]. For relatively thick films, the initial bicontinuous pattern experiences axisymmetric hole expansion in the valleys and minor fragmentation of hills. Subsequent hole coalescence eventually leads to the formation of polygonal structures resembling Voronoi tessellations. A different behavior arises for thinner films, where the bicontinuous pattern directly fragments to form isolated droplets [8]. The transition between the two morphological pathways seems to occur close to the minimum of the film diffusivity $\partial^2\Delta G/\partial h^2$ curve.

3. Experimental details

Through the fragile interaction of several parameters, including surface morphology, surface termination, open dangling bonds, and the presence of a water layer obstructing/complicating the exact prediction of results by theoretical calculation, our experiments provide unambiguous means of determining optimal conditions (controlling the dewetting pathway) for the formation of small dots for future experiments.

To experimentally investigate the influence of dewetting parameters on the evolution of film morphology, platinum films with a thickness of 1.5, 3, 7, and 15 nm were prepared by electron-beam evaporation (base pressure 2×10^{-6} mTorr (3×10^{-9} mbar), deposition rate 0.2–0.4 nm s^{-1}) onto a silicon (100) substrate containing a natural oxide layer. For each thickness, samples were processed in a rapid thermal processing (RTP) oven (RTP-600s, Modular Process Technology Corp., San Jose, CA, USA) at temperatures of 400, 500, 600, 700, 800, and 1000 °C for 30, 90, and 240 s. During this process, the samples were placed on a silicon carbide chuck and heated by radiation with halogen lamps. The annealing procedure consisted of the following steps: (1) load RTP chamber with samples; (2) flush chamber for 20 s with nitrogen at 20 slpm (liters per minute at standard conditions); (3) flush nitrogen for 5 s at 2 slpm; (4) raise and maintain a constant temperature via feedback control with a thermocouple sensor for the chosen annealing time; (5) stop heating while flushing with nitrogen to allow the sample to cool. The furnace was opened after the temperature had dropped below 100 °C. Subsequently, the samples were imaged with a scanning electron microscope (Raith 150, Zeiss Gemini Column, acceleration voltage 10 kV, working distance approximately 7 mm).

To demonstrate the suitability of the prepared structures for further processing, samples with 3 nm thick platinum film, dewetted at 800 °C for 240 s, were subsequently processed by reactive ion etching (RIE, Plasma-Therm, 700 series) to form a three-dimensional nanostructured surface. A two-step RIE process was used, whereby samples were (1) etched for 1 min with BCl_3 (RF-power 150 W, pressure 20 mTorr (3×10^{-2} mbar), gas-flow 20 sccm) and (2) etched for 3 min with Cl_2 (RF-power 150 W, pressure 30 mTorr (4×10^{-2} mbar), gas-flow 20 sccm). The etched samples were imaged with the scanning electron microscope.

4. Results and discussion

To relate the evolution of film morphology to theoretical pathways and to pinpoint which parameters yielded the smallest features, images of samples processed at different film thickness, temperature, and time were taken and compared. Figures 1 and 2 show scanning electron micrographs presenting the evolution of film morphology over a range of thicknesses and temperatures for an annealing time of 30 and 240 s. The figures highlight the influence of annealing time on the dewetting pattern. In figures 1 and 2, similar patterns can be recognized, but at different temperatures.

Rows represent the film thicknesses of 1.5, 3, 7, and 15 nm and columns display the initial samples and samples processed at annealing temperatures between 400 and 1000 °C. All images are presented in identical magnification, except the right lower corners (separated by a black line) are displayed with a larger field of view due to the increased dimensions of the features.

We observed film evolution from bicontinuous pattern formation via droplet formation, to droplet coarsening for samples with a 1.5 and 3 nm thick platinum film.

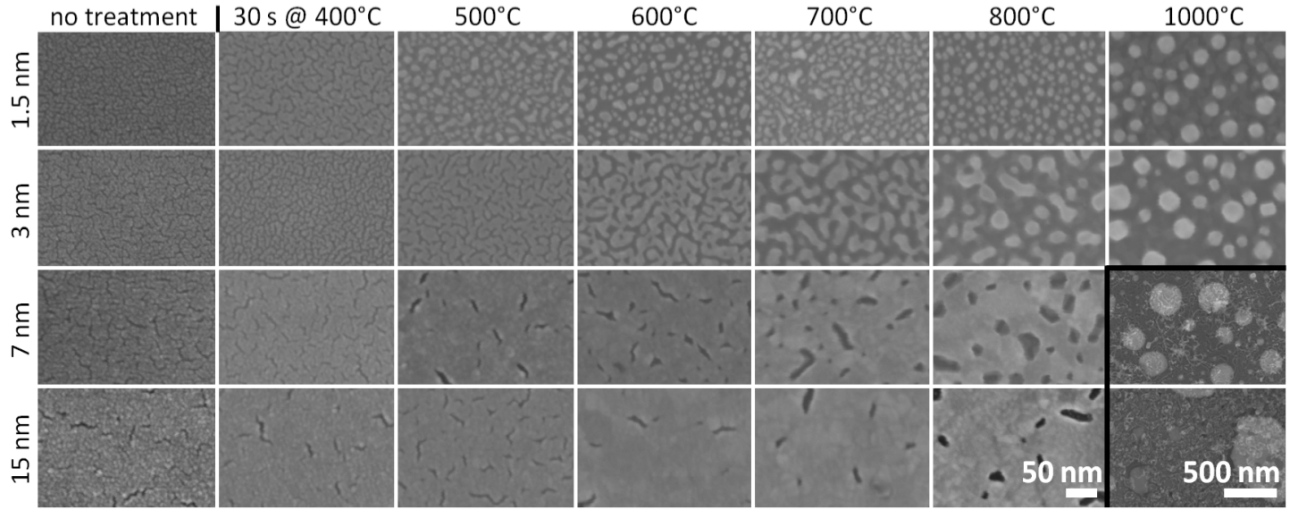

Figure 1. SEM micrographs displaying the evolution of film morphology of platinum-thin-films of 1.5, 3, 7, and 15 nm annealed at 400–1000 °C for 30 s. Since no adhesion layer was used below platinum, the non-treated films already exhibit post-deposition cracks to lower their free energy. At low temperatures, the 1.5 nm (400 °C) and 3 nm (400–700 °C) Pt films showed a fragmented, bicontinuous–spinodal pattern, evolving to droplet formation with increased temperature (500 and 800 °C). The thicker platinum films 7 and 15 nm exhibited hole formation and expansion of holes. In addition, on these thicker films a platinum silicide formation was observed at higher temperatures (700 °C and above). The images in the right lower corner—separated by the black line—are presented with lower magnification to show their large structures (scale bar 500 nm).

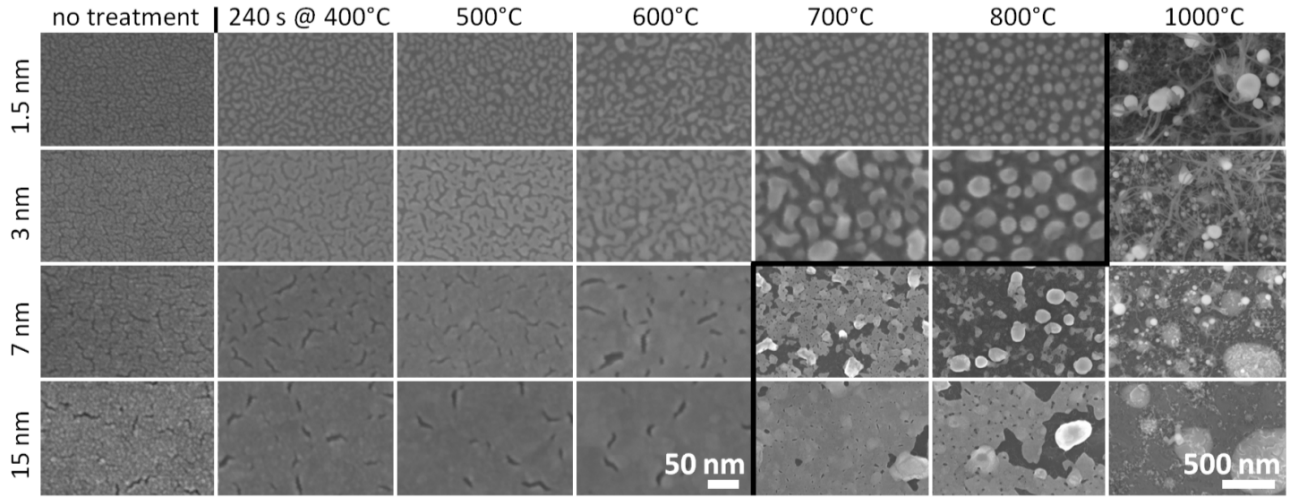

Figure 2. SEM micrographs displaying the evolution of film morphology at an increased annealing time of 240 s. They depict the change in pattern for longer annealing time as compared to figure 1 (annealing time 30 s). For an annealing time of 240 s, the coalescence towards droplets was further developed for the thinner films (1.5 and 3 nm). For thicker films (7 and 15 nm), hole expansion in combination with dot formation was observed at 700 °C, indicating a different pathway of droplet formation. At 1000 °C, nanowire growth was observed for 1.5 and 3 nm thick films, whereas for 7 and 15 nm thick films platinum silicide islands formed. The images on the right side—separated by the black line—are presented with lower magnification to show their large structures (scale bar 500 nm).

Analyzing the images, it is clear that the thickness of these films was below the thickness necessary to form a stable coverage of the surface during dewetting. At 500 °C and 30 s annealing time (figure 1), the bicontinuous–spinodal pattern of the 1.5 nm thick platinum films had already fragmented into isolated clusters (droplets) and each successive temperature increase resulted in further coalescence until circular droplets formed at 800 °C. For 3 nm films, the fragmentation process started at higher temperature 600 and 700 °C and circular drops had not yet formed at 800 °C.

The influence of the thin oxide coating of the substrate (natural oxide layer of silicon) was apparent in the formation of droplets directly from the bicontinuous pattern. Without this coating, the sole option in an exclusively apolar system subjected to long-range Lifshitz–van der Waals attraction is axial-symmetric hole expansion following the early stage spinodal pattern [8].

In contrast, the thicker 7 and 15 nm films followed different evolutionary pathways. Two pathways were found within our results. Sharma and Khanna describe one universal

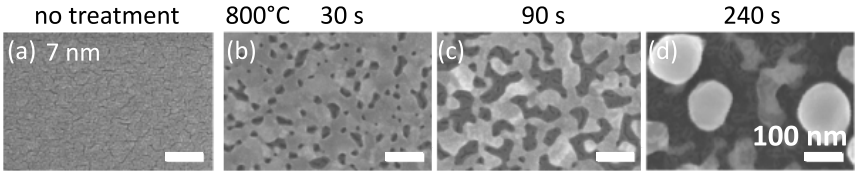

Figure 3. Influence of dewetting time on a platinum-thin-film (7 nm, 800 °C) on silicon with natural oxide: before treatment (a) and annealed for 30, 90, and 240 s ((b)–(d)). First bicontinuous hole formation appeared for an annealing time of 30 s, followed by a coalescence process ((b)–(c)). At the longest annealing time, the coalescence process of material from thinner towards thicker areas finally led to separated metal droplets (d). Whereas at 90 s annealing time, no droplet formation was found at all. After 240 s annealing time, the holes had interconnected and the metal had agglomerated into droplets. Image (c), shows a multilayer structure composed of apparently disparate materials. Analysis of these structures suggest that this multilayer structure was caused by the formation of different platinum silicide (PtSi) phases. Scale bars are each 100 nm.

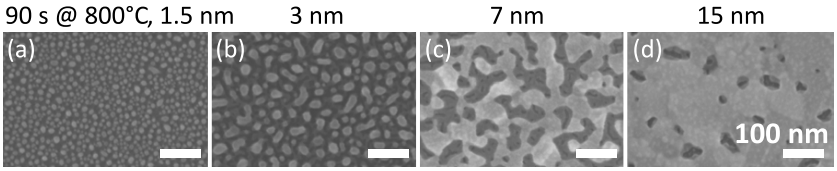

Figure 4. Influence of film thickness on dewetting pattern. Platinum layers of 1.5, 3, 7, and 15 nm thickness were annealed at 800 °C for 90 s. For the 1.5 and 3 nm thick layers, the initial metal film had already fragmented into droplets at 800 °C. For the 7 and 15 nm thick layers, hole formation had started, whereas for an annealing time of 90 s, the progression to droplets had not yet begun. Scale bars are 100 nm.

path of evolution as subject to hole expansion following the early stage spinodal pattern [8]: holes coalesce together and islands of metal remain. We relate the smaller, nearly circular holes observed e.g. in figure 1: annealing time 30 s, 7 nm–600 °C and 15 nm–700 °C to an early stage of this pathway for film evolution. It should be mentioned that the axial-symmetric holes experienced in Sharma's simulations resulted from ideal conditions not present under our non-ideal experimental conditions (e.g. they do not consider physical/chemical heterogeneities and post-deposition stress in the film). We hypothesize that these non-idealities resulted in non-axial-symmetric holes in our experiment. Dewetting by spinodal hole formation was also observed by Bischof *et al* upon dewetting a 47 nm thick Au film from a fused silica substrate [6].

The second pathway of dewetting also begins solely by hole formation, whereas for higher temperatures a coexistence of single drops mainly surrounded by a thin film becomes prominent (figure 2: annealing time 240 s, 7 nm–700 °C and 15 nm–800 °C). An earlier stage of this development is visible in figure 2 (15 nm–700 °C), where the neighboring areas have not yet completely thinned out and the droplets are still connected to the surrounding metal film.

Figure 3 shows the evolution of a 7 nm thick platinum for different dewetting times. For an annealing time of 90 s, a bicontinuous structure composed of long hills and valleys persists until the fragmentation of hills directly produces an array of droplets (figure 3(c)). The result for longer dewetting time is shown in figure 3(d). By increasing the dewetting time, a transition from interconnected networks to separated individual droplets occurred. The droplets become increasingly circular due to surface tension and increase in height due to flow from the valleys which thin and flatten out. Thus, pseudo-dewetting occurs by retraction of droplets, rather than by the expansion of holes.

The effect of varying film thickness on film pattern for identical processing parameters is shown in figure 4. Additionally, it can be studied by following the columns in figures 1 and 2. Examining the 1.5 and 3 nm thick films in figure 4, we once again observed that the initial film had fragmented and already formed separated droplets. The 7 nm thick films exhibited a multilayered geometry composed of apparently disparate materials (figure 4(c)). Such layered geometry was explained by Sekhar as the formation of various PtSi phases as the film exceeded certain temperatures [12], in our case 700 °C. Finally, the 15 nm film exhibited an early stage of pseudo-dewetting, the formation of droplets due to material concentration by retraction, rather than expansion of holes (d).

Three different behaviors were identified for interdiffusion of Pt and silicon during our study: (1) formation of PtSi layers at lower temperatures and at 1000 °C either (2) nanowire growth in thinner films or (3) formation of PtSi islands (on top or within the surface) in thicker films. All three cases coincide with Sekhar's observations [12].

At a temperature around 300 °C, interdiffusion of Pt in Si may produce Pt2Si [12]. The heterogeneity introduced upon formation of Pt2Si at lower temperatures may explain the simultaneous presence of 'spinodal holes' (smaller holes) and nucleation-driven holes (irregular larger holes), as witnessed in 7 nm films in figure 2 at 600 °C. This simultaneous presence of different hole types is also observed for thicker films but at higher temperatures (figure 2, 15 nm, 700 °C).

If the processing temperature is increased to 1000 °C, the growth of silicon nanowires may be catalyzed by silicide formation on thinner platinum films (figure 5(a) as well as figure 2: 1.5 and 3 nm at 1000 °C). The underlying mechanism

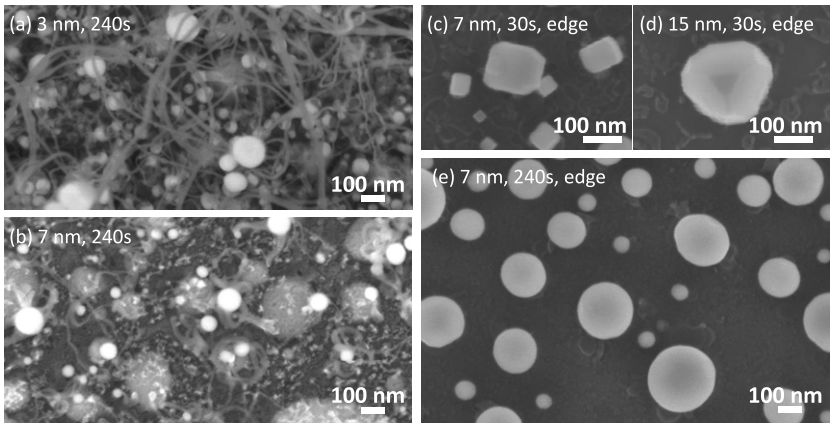

Figure 5. SEM images of samples processed at 1000 °C. (a) Sample with 3 nm platinum-thin-film dewetted for 240 s annealing time. Within 3 nm films, silicide formation may catalyze the growth of silicon nanowires by the formation of a vapor phase on the sample surface. (b) No nanowire growth was found for 7 nm platinum films. Instead PtSi islands formed. (c) and (d) SEM images were taken at a position close to the edge of samples with 7 and 15 nm platinum-thin-film annealed for 30 s each. Here, faceted structures are visible on the surface, which can be explained by the formation of the crystalline material platinum silicide. If these crystals are heated for a longer period, circular droplets form instead (e).

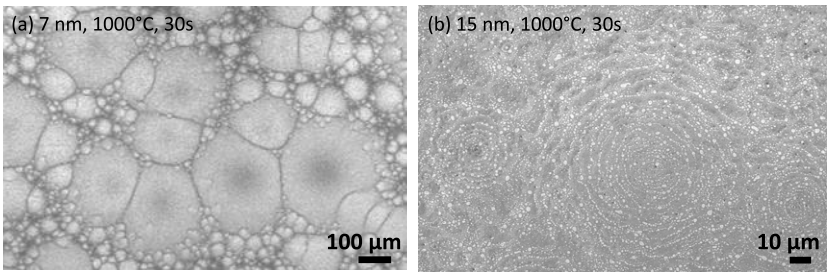

Figure 6. (a) SEM image of a 7 nm platinum-thin-film annealed at 1000 °C for 30 s, showing polygonal networks. (b) 15 nm film with secondary multi-ring structures decomposed into droplets via Rayleigh instability.

of this catalysis is explained by the vapor liquid solid (VLS) growth model [12], by which increased temperatures create Si vapor which is swept across the substrate by a carrier gas (N_2 in our thermal annealing system). This sweeping induces a whiskering effect that produces the Si nanowires.

On the other hand, thicker films inhibit nanowire growth and large islands of PtSi may form instead at 1000 °C, as visible in figure 5(b) for a 7 nm film. Close to the edge of these 7 and 15 nm Pt samples, PtSi crystalline islands formed on top of the surface, observed as faceted structures in images (c) and (d). Auger spectroscopy confirmed the presence of both Pt and Si in these islands. If the 7 and 15 nm Pt samples are heated for a longer period nearly spherical droplets were observed (e).

In thermal dewetting of thin films not only short-range but also long-range ordering effects can appear. We encountered such long-range effects during our dewetting experiments. Figure 6(a) shows a 7 nm thick film annealed at 1000 °C for 30 s. The film with an initial thickness above the threshold for spinodal dewetting formed polygonal networks. The networks are reminiscent of the description of Sharma and Khanna [8], however at different length scale. Another example of long-range dewetting behavior is given in figure 6(b) which presents the annealing results of a 15 nm thick Pt film at 1000 °C for 30 s. In this image several concentric rings can be identified, which are fractured into small droplets. This circular morphology was also encountered by Kargupta and Sharma by simulation of heterogeneous substrates [11]. They found that physicochemical heterogeneities may instigate the growth of secondary multi-ring structures surrounding them, which then decompose into droplets via Rayleigh instability.

The wide range of behaviors presented here illustrates the multiple factors which must be considered when attempting to control morphology via thermal dewetting. Therefore, conducting experiments to study the dewetting behavior is the least ambiguous approach. In our experiments, we found that in samples annealed at 1000 °C, various material interactions result in both desired and undesired behavior. In addition, one must minimize heterogeneities present in the system to obtain a homogeneous pattern on the longer length scale.

The smallest structures with a mean diameter of about 9 nm were obtained for 1.5 nm thick platinum films annealed at 800 °C for 30 s (figure 7 inset). Figure 7 shows the histogram of the major axis of the droplets (end-to-end lengths) for different initial film thicknesses and annealing times. The histogram plots the number of colloids within a certain end-to-end length range (1 nm raster) normalized to 1 by dividing through total counts versus the logarithm of the end-to-end

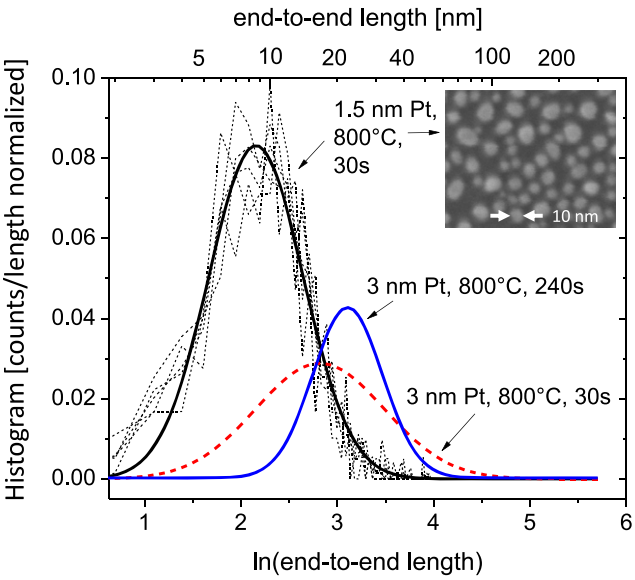

Figure 7. Histogram of the diameter of the dewetting droplets (end-to-end length) analyzed for different initial film thicknesses and annealing times. The samples with 1.5 nm platinum dewetted at 800 °C for 30 s showed the smallest features with a mean length of about 9 nm obtained by a Gaussian fit. The histograms of four individual measurements are shown as dashed lines, the natural log (ln) Gaussian fit of their average as a line, and for comparison, the ln Gaussian fits for 3 nm samples dewetted at 800 °C for 30 and 240 s (mean diameter 17 and 22 nm). Inset: SEM image of a 1.5 nm thick platinum film dewetted at 800 °C for 30 s.

(This figure is in colour only in the electronic version)

length. In this logarithmic plot, the mean of end-to-end length was determined by a Gaussian fit. The 1.5 nm thick platinum films annealed at 800 °C for 30 s revealed a mean-structure length of about 9 nm. As described in the above-mentioned theory, these structures were formed by dewetting via droplet formation directly following bicontinuous pattern formation.

Larger dewetting structures were obtained if a platinum layer with a thickness of 3 nm was used. A mean diameter of 17 nm was obtained by annealing 3 nm thick platinum films for 30 s (figure 1: 3 nm, 800 °C). Annealing of 3 nm films for 240 s resulted in structures with an average diameter of 22 nm (figure 2: 3 nm, 800 °C). Due to the increased annealing time, the metal had more time to coalesce (30–240 s). Thus, we observed a larger mean diameter in combination with a narrower distribution, whereas no significant additional coalescence was observed for 1.5 nm thick films processed for an annealing time of 240 s instead of 30 s.

To demonstrate the utilization of the obtained dewetting pattern as an etch mask, it was transferred by reactive ion etching into the underlying silicon substrate. We chose a sample with a 3 nm thick platinum layer dewetted at 800 °C for 240 s, see figure 2. After etching, a network of 150 nm tall interconnected nanopillars with a top diameter of roughly 35 nm was obtained, as shown in figure 8. This high aspect ratio was possible due to the etch process with BCl_3 and Cl_2 gases which resulted in an anisotropic etch behavior. The 3 nm thick platinum film was chosen for etching, to ensure adequate stability of the structures, although we believe the 1.5 nm samples could also be successfully processed, and should result in even smaller structures.

5. Conclusion

We have characterized the dewetting behavior of platinum on silicon for 1.5–15 nm thick films annealed at 400–1000 °C for 30 and 240 s. The observed morphological evolution of the processed films corroborates theoretical simulations of dewetting and helps dispel the belief that hole formation always indicates the nucleation mechanism. We determined the processing parameters 800 °C and 30 s for a 1.5 nm thick platinum film, resulting in structures with a mean end-to-end length of 9 nm. In addition, the nanostructures were successfully applied as an etch mask for subsequent reactive ion processing to fabricate tapered silicon nanopillars. The presented results provide a guide to the morphological evolution of thin films which can be used to tailor future experiments to produce desired features. Future research will aim to extend the parameters to even thinner films and to apply the knowledge about pattern morphology of thermally dewetted metal films toward applications in other areas such as the templating of self-assembly systems.

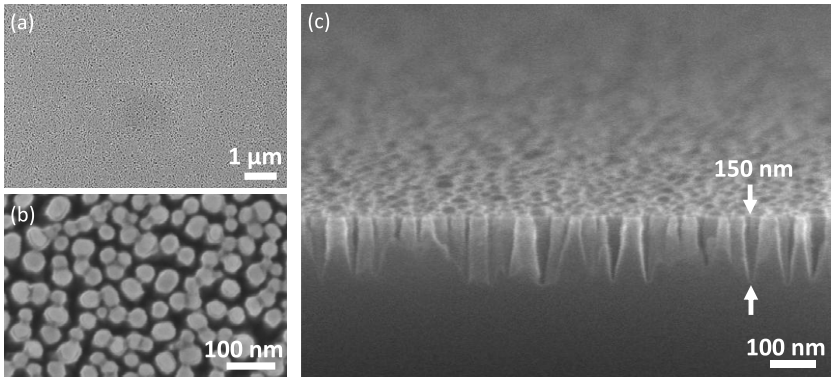

Figure 8. SEM images of a sample where the dewetted thin film (3 nm Pt, 800 °C, 240 s) was used as a mask for reactive ion etching. Images (a) and (b) show top views, and (c) shows a cross section at an angle close to 90°. By etching with BCl_3 and Cl_2, a network of 150 nm tall partially interconnected nanopillars was formed. Depending on the thermal processing parameters single non-connected pillars can also be formed.

Acknowledgments

Many thanks are given to Joshua Leu for his help and discussions on image analysis of the samples and to Jim Daley and Mark Mondol for their help with fabrication and imaging. In addition, the support of the MSRP staff was integral in carrying out the research. Electron-beam lithography was done in MIT's shared Scanning-Electron-Beam-Lithography (SEBL) facility in the Research Laboratory of Electronics. One of the authors (JC) was supported through a Samsung fellowship and by the ONR. We acknowledge financial support from the Alfaisal University and the King Abdulaziz City for Science and Technology.

References

[1] Vrij A 1966 Possible mechanism for spontaneous rupture of thin free liquid films *Discuss. Faraday Soc.* **42** 23
[2] Becker J *et al* 2003 Complex dewetting scenarios captured by thin-film models *Nat. Mater.* **2** 59–63
[3] Lee J and Kim B 2007 Thermal dewetting of Pt thin film: etch-masks for the fabrication of semiconductor nanostructures *Mater. Sci. Eng.* A **449** 769–73
[4] Lee Y, Koh K, Na H, Kim K, Kang J and Kim J 2009 Lithography-free fabrication of large area subwavelength antireflection structures using thermally dewetted Pt/Pd alloy etch mask *Nanoscale Res. Lett.* **4** 364–70
[5] Van Oss C, Chaudhury M and Good R 1988 Interfacial Lifshitz–van der Waals and polar interactions in macroscopic systems *Chem. Rev.* **88** 927–41
[6] Bischof J, Scherer D, Herminghaus S and Leiderer P 1996 Dewetting modes of thin metallic films: nucleation of holes and spinodal dewetting *Phys. Rev. Lett.* **77** 1536
[7] Seemann R, Herminghaus S and Jacobs K 2001 Dewetting patterns and molecular forces: a reconciliation *Phys. Rev. Lett.* **86** 5534–7
[8] Sharma A and Khanna R 1998 Pattern formation in unstable thin liquid films *Phys. Rev. Lett.* **81** 3463–6
[9] Sharma A and Khanna R 1999 Pattern formation in unstable thin liquid films under the influence of antagonistic short- and long-range forces *J. Chem. Phys.* **110** 4929–36
[10] Khanna R and Sharma A 1997 Pattern formation in spontaneous dewetting of thin apolar films *J. Colloid Interface Sci.* **195** 42–50
[11] Kargupta K and Sharma A 2002 Creation of ordered patterns by dewetting of thin films on homogeneous and heterogeneous substrates *J. Colloid Interface Sci.* **245** 99–115
[12] Sekhar P, Sambandam S, Sood D and Bhansali S 2006 Selective growth of silica nanowires in silicon catalysed by Pt thin film *Nanotechnology* **17** 4606–13